PHYSICAL REVIEW A **110**, 022805 (2024)

Low-energy positron scattering by saturated and unsaturated hydrocarbons: Cross sections and bound states

Francisco Fernandes Frighetto, Sergio d'Almeida Sanchez, and Alessandra Souza Barbosa[*]
Departamento de Física, Universidade Federal do Paraná, Caixa Postal 19044, 81531-980 Curitiba, Paraná, Brazil

(Received 27 March 2024; revised 23 May 2024; accepted 17 July 2024; published 8 August 2024)

We employed our recent version of the Schwinger multichannel method, implemented with a model potential [F. F. Frighetto, A. S. Barbosa, and S. d'A. Sanchez, Phys. Rev. A **108**, 012818 (2023)] to calculate cross sections for elastic positron scattering by a set of hydrocarbons. Initially, by comparing the model potential calculations for methane, ethylene, and acetylene with our best possible *ab initio* calculations to date, we obtained the cutoff parameter for the carbon atom. Our results show that this parameter depends on the hybridization of the carbon atom for each molecule. We then applied the same cutoff parameter for the model potential to calculate the cross sections for other saturated and unsaturated hydrocarbons with encouraging results. We also discuss the positron binding to these hydrocarbons and compare the present results with available data from the literature.

DOI: 10.1103/PhysRevA.110.022805

I. INTRODUCTION

Understanding positron interactions with matter is of significant importance for many applications spanning interstellar physics [1,2], condensed-matter physics [3–6], and medical imaging, as in positron emission tomography [7,8]. Therefore, there is an urgent need to study the interaction of positrons with molecules, from the smaller and simpler ones (such as hydrogen, nitrogen, and methane) to the bigger and more complex systems (for example, hexane, benzene, and even DNA basis).

Despite the evident importance of positron-molecule studies, there are many difficulties for both theoretical and experimental groups to fully understand low-energy (typically below 10 eV) positron scattering. In experiments, limitations in the angular resolution of the experimental apparatus seem to be the main cause for the discrepancy among measurements from different groups. In theoretical studies with *ab initio* methods, such as Schwinger multichannel (SMC) method [9,10], R matrix [11–13], convergent close coupling (CCC) [14], and many-body theory (MBT) [15,16], the difficulties arise from accurately accounting for positron-molecule correlation-polarization interactions, even for small molecules.

Usually, what is observed in the comparison of the calculated elastic-scattering data with experiments is that the former significantly underestimates the experimental results even when the positronium (Ps) formation channel is closed [13,17–21]. Some hypotheses raised on why this happens are (i) lower than expected intensity of the calculated differential cross sections (CSs) in smaller angles ($\theta < 30^\circ$) [13], (ii) poor description of the correlation polarization of the target's electrons due to the incoming positron [13,17–21], and (iii) the difficulty in obtaining the experimentally observed positron-molecule bound states for nonpolar molecules [15,21–25], sometimes even identified as virtual states [18–20]. It is also worth mentioning recent calculations for H_2 from Zammit *et al.* [14] with CCC, and H_2, N_2, and CH_4 from Rawlins *et al.* [16], with MBT that have in fact provided a much better agreement with the experimental data when compared to other calculations. Nonetheless, some of the issues still persist, as the differential cross sections (DCSs) of Zammit *et al.* [14] for H_2 still do not capture perfectly the low angle region ($<30^\circ$) from the experimental DCS of Machacek *et al.* [26]. Furthermore, even though the MBT results of Rawlins *et al.* [16] have an excellent agreement with experiments, their data are limited to ICS and to impact energies below 2.0 eV for N_2 and CH_4, due to computational costs.

On top of all these issues, the expensive cost associated with performing *ab initio* calculations for large molecules makes the study of these types of systems either flawed, due to the lack of an accurate description of the positron-molecule correlation-polarization interactions, or unfeasible at the current time. In this context, the use of a model potential for cross-section calculations is very interesting, especially if the model potential is able to reproduce earlier successful *ab initio* results for the cross sections of small molecules and is able to predict cross sections for larger systems.

Recently, we have implemented the model potential proposed by Swann and Gribakin [27], for positron binding calculations, in our Schwinger multichannel method codes for positron scattering calculations [28]. In particular, we have shown that the model potential was able to reproduce the fully *ab initio* results for the diatomic molecules H_2 and N_2, and found the cutoff radius (a free parameter of this model potential) that better fitted the *ab initio* results. Following this study, we now raise our attention to obtain calculated cross sections for saturated and unsaturated hydrocarbon molecules. Initially, we aim to show that the calculations in the static plus model potential approximation ($S + V_{CP}$) reproduce our high-level static plus polarization (SP) results, recently obtained for

---

[*] Contact author: alessandra@fisica.ufpr.br

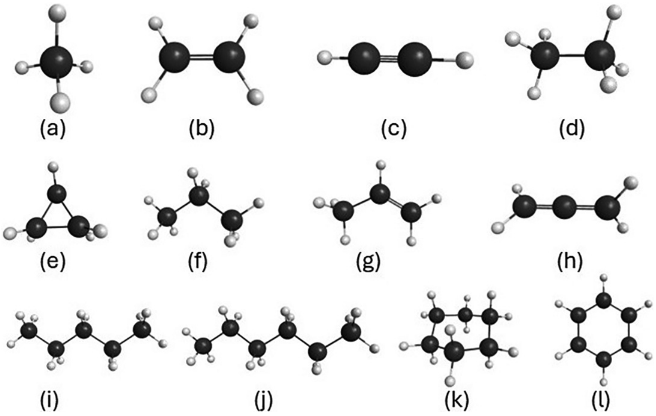

FIG. 1. Geometrical structure of the molecules studied in this paper: (a) methane, (b) ethylene, (c) acetylene, (d) ethane, (e) cyclopropane, (f) propane, (g) propene, (h) allene, (i) *n*-pentane, (j) *n*-hexane, (k) cyclohexane, and (l) benzene.

methane, ethylene, and acetylene [29]. Then, to ensure the ability to predict results within the $S + V_{\mathrm{CP}}$ approximation, we present calculated cross sections for the bigger alkane and cycloalkane molecules ethane, propane, cyclopropane, *n*-pentane, hexane, and cyclohexane, and for the alkenes and alkynes molecules allene, propyne, propene, and benzene. The geometrical representation of all molecules studied here is shown in Fig. 1.

The main reasons for choosing these systems for this test are due to the availability of experimental data for all molecules [30]. Besides that, previous calculations for some of the molecules [19–21,31] were unable to accurately describe the existing experimental data for some of these systems, providing an opportunity to improve the calculated theoretical results. It is also worth mentioning that only with this methodology it was possible to calculate reliable cross sections for bigger molecules like pentane, cyclohexane, and hexane.

This paper will be organized as follows: in Sec. II we will briefly describe the SMC method, in Sec. III we present the calculated results for the integral cross section (ICS), DCSs, and virtual or bound-state energy for positron elastic scattering from the systems of interest, and in Sec. IV we give some concluding remarks about the results.

II. THEORY

A. Schwinger multichannel method

The Schwinger multichannel method [9,10] has already been described in detail in other works, in such a way that we will only review the most important aspects of the method. The resulting scattering amplitude from the Schwinger multichannel method for positron scattering from molecules or atoms has the following form:

$$f_{\mathrm{SMC}}(\vec{k}_f, \vec{k}_i) = -\frac{1}{2\pi} \sum_{\mu,\nu} \langle S_{\vec{k}_f} | V | \chi_\mu \rangle (d^{-1})_{\mu\nu} \langle \chi_\nu | V | S_{\vec{k}_i} \rangle \quad (1)$$

where

$$d_{\mu\nu} = \langle \chi_\mu | Q\hat{H}Q + PVP - VG_p^{(+)}V | \chi_\nu \rangle. \quad (2)$$

In the above expressions, P is the projection operator onto energetically open electronic states of the target (in the present calculations, only the elastic channel is open and, therefore, $P = |\Phi_0\rangle\langle\Phi_0|$); Q is the projection operator onto energetically closed electronic states of the target; $\hat{H}$ is the collision energy minus the full scattering Hamiltonian; $G_P^{(+)}$ is the free-particle Green's function projected on the P space; $|S_{\vec{k}_{i(f)}}\rangle$ is a solution of the unperturbed Hamiltonian H_0 and is given by the product of a target state and a plane wave with momentum $\vec{k}_{i(f)}$; V is the interaction potential between the incident positrons and the electrons and nuclei of the target. Finally, $|\chi_\mu\rangle$ is an $(N+1)$-particles (N electrons and one positron) variational trial basis. Within the Schwinger multichannel method, the positron-molecule interactions can be treated in the static (S), SP, and $S + V_{\mathrm{CP}}$ approximations. In this paper, we will focus our calculations on the $S + V_{\mathrm{CP}}$ approximation.

In the $S + V_{\mathrm{CP}}$ approximation [28], instead of using virtual excitations to include the correlation-polarization interactions between the incident positron and the electrons of the target molecule, these interactions are explicitly included through the model potential, V_{CP}, proposed by Swann and Gribakin [23,27,32], resulting in the following expression for the scattering amplitude:

$$f_{\mathrm{SMC\text{-}CP}}(\vec{k}_f, \vec{k}_i) = -\frac{1}{2\pi} \sum_{\mu,\nu} \langle S_{\vec{k}_f} | (V + V_{\mathrm{CP}}) | \chi_\mu \rangle (d^{-1})_{\mu\nu} \times \langle \chi_\nu | (V + V_{\mathrm{CP}}) | S_{\vec{k}_i} \rangle, \quad (3)$$

where

$$d_{\mu\nu} = \langle \chi_\mu | Q\hat{H}Q + P(V + V_{\mathrm{CP}})P - (V + V_{\mathrm{CP}})G_p^{(+)}(V + V_{\mathrm{CP}}) | \chi_\nu \rangle. \quad (4)$$

The explicit form of the model potential is given by

$$V_{\mathrm{CP}}(\vec{r}) = \sum_A V_{\mathrm{CP}}^{(A)}(\vec{r}) = -\sum_A \frac{\alpha_A}{2|\vec{r} - \vec{r}_A|^4} \left[1 - \exp\left(-\frac{|\vec{r} - \vec{r}_A|^6}{{\rho_A}^6} \right) \right], \quad (5)$$

where A is the index representing the atoms of the molecule, α_A are the hybrid polarizabilities of atom A according to the work of Miller [33], and ρ_A is the empirical parameters of the model potential for atom A.

Since polarization effects are taken into account through the model potential V_{CP}, we kept the molecular orbitals frozen through, just as in the S approximation.. The fact that we describe the target as in the S approximation makes it possible for the use of all configuration state functions (CSFs) associated with the ground state of the molecule in the calculations within the $S + V_{\mathrm{CP}}$ approximation. It is also worth mentioning that any inelastic processes are not included in the present calculations.

B. Computational details

In the calculations carried out for methane, acetylene, ethylene, ethane, propene, cyclopropane, and benzene molecules, we have employed the molecular geometries from the previous SMC-SP calculations [20,21,29]. For propyne, propane,

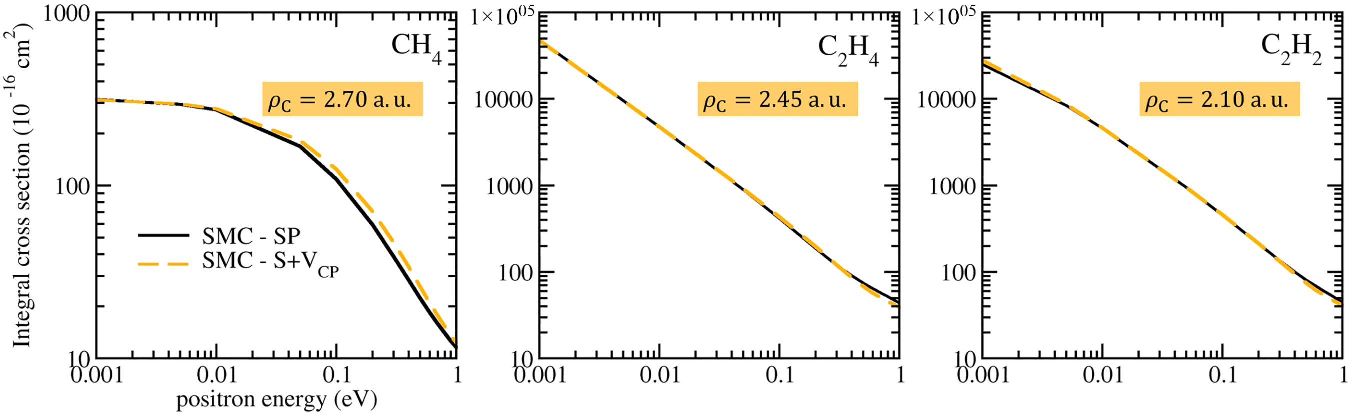

FIG. 2. ICS for positron scattering from methane (left), ethylene (center), and acetylene (right). Our previous SP calculations [29] (solid black line) are compared with present $S + V_{\mathrm{CP}}$ calculations (dashed orange line), in order to determine the optimal ρ_C for each carbon atom hybridization. See text for discussion.

n-pentane, cyclohexane, and hexane, which are studied theoretically here, we have employed the experimental geometries [34]. Despite the fact that the chain alkanes *n*-pentane and *n*-hexane present more than one stable conformer [35], here we present results only for the most stable conformation of both molecules. We have exploited the molecular symmetry in the scattering calculations for all molecules. In some cases, when the molecule belongs to a non-Abelian symmetry group, the calculation was carried out in an Abelian subgroup (e.g., methane belongs to the non-Abelian T_d group but the scattering calculations were carried out in the C_{2v} Abelian group). The $TZV++(3d, 3p)$ basis set was employed in the atomic centers of most molecules studied here, except for *n*-pentane, hexane, and cyclohexane where the $TZV++(2d, p)$ basis set was employed.

As will be discussed in the next section, in the $S + V_{\mathrm{CP}}$ approximation calculations done in this paper, we have employed different cutoff parameters ρ for each atom and hybridization. For the hydrogen atoms, we have used $\rho_H =$ 1.90 a.u., obtained from our previous work [28]. For the carbon atoms, we have found the cutting distances $\rho = 2.70$ a.u. for the sp_3 hybridization, $\rho = 2.45$ a.u. for the sp_2 hybridization, and $\rho = 2.10$ a.u. for the sp hybridization, since these best fitted our very-low-energy *ab initio* results for the methane, acetylene, and ethylene molecules [29].

III. RESULTS AND DISCUSSIONS

Our calculated ICS and DCSs or folded differential cross sections are presented here. Initially, we will present the results for methane, acetylene, and ethylene, in order to find the optimal cutoff radius for the carbon atom in each hybridization. This will be done by comparing our model potential calculations with our previous high-level SP calculations for those systems. Then we will exploit the model potential calculations to bigger hydrocarbons, by employing the cutoff radius found previously. Finally, we will close this section with a discussion on the *s*-wave eigenphases, scattering lengths (SLs), and virtual or bound-state energies obtained from the calculations with the SMC method in the $S + V_{\mathrm{CP}}$ approximation.

A. Finding the optimal ρ

In order to successfully apply the model potential in calculating cross sections for positron scattering for bigger hydrocarbons, we first need to determine the cutoff parameter of the potential for every atom. As mentioned earlier, the hybrid polarizations α_A from Eq. (5) were taken from [33]. For the cutoff parameter ρ_A, the best approach is to determine the value that fits our high-level SP calculations for small systems and, then, use the same value in calculations for bigger molecules. It is worth mentioning that this parameter is different for each atom and can also be different depending on the atom's hybridization.

In Fig. 2 we compare our most recent elastic ICS, obtained in the static plus polarization approximation [29], with the present $S + V_{\mathrm{CP}}$ results that best fitted our SP data, for methane, ethylene, and acetylene. For the hydrogen atom, we have employed $\rho_H = 1.90$ a.u., as found recently [28], whereas for carbon atoms we have observed that different values of ρ_C are required for different C hybridization. In particular, we have focused on determining the optimal ρ value in order to fit our SP results for impact energies up to 1.0 eV. For methane, the simplest alkane molecule, we have found the cutoff parameter for the C atom of 2.70 a.u., whereas for ethylene and acetylene, the simplest alkene and alkyne, respectively, the optimal ρ_C was 2.45 and 2.10 a.u., respectively. In Table I, we summarize the values for ρ and α_A for each atom and hybridization employed in these calculations.

As discussed in our previous work [28], the smaller (bigger) the cutoff parameter ρ the more (less) attractive the

TABLE I. Parameters of the model potential employed in the scattering calculations

Atom	α_A (a.u.) [33]	ρ (a.u.)
H	2.612	1.90 [28]
C (sp_3)	7.160	2.70
C (sp_2)	9.124	2.45
C (sp)	8.658	2.10

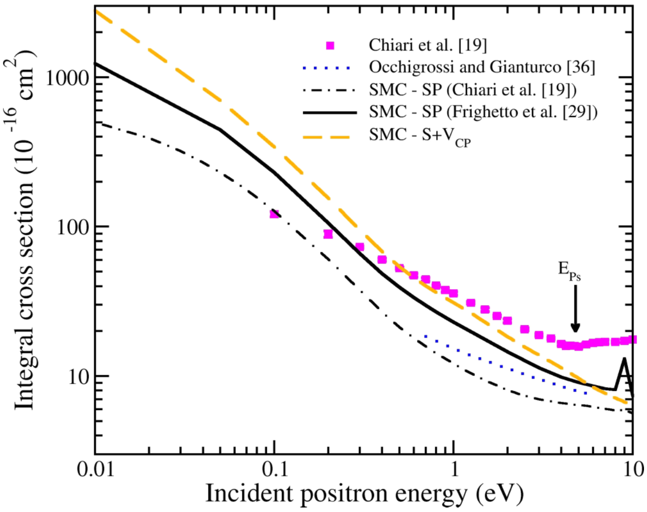

FIG. 3. ICS for elastic positron scattering from ethane. Our $S + V_{\mathrm{CP}}$ (orange dashed line) results are compared with the experimental data and SMC-SP calculations of Chiari *et al.* [19] (magenta circles), the early calculations of Occhigrossi and Gianturco [36] (dotted blue line), and more recent SMC-SP calculations of Frighetto *et al.* [29] (solid black line). The downwards arrow corresponds to the energy at which the positronium channel opens ($E_{\mathrm{Ps}} = 4.8$ eV [19])

model potential V_{CP}. For example, from Table I it is noted that V_{CP} is more attractive for the carbon atom in the sp_2 hybridization and less intense for the sp_3 hybridization. This result corroborates previous theoretical and experimental works that argue that the binding energy increases when the molecular target presents π bonds [15,24]. The π orbitals are more localized in the atoms, screening the repulsive potential of the nuclei experienced by the positron. This would make the electrons more accessible for the incident positron, resulting in a more intense interaction between the positron and the electrons of the molecule [15,24].

B. Applications

After determining the cutoff parameter for the hydrogen atom [28], and for each hybridization of the carbon atom, it becomes imperative to assess the accuracy of $S + V_{\mathrm{CP}}$ approximation in calculations for larger molecules, employing these cutoff parameters. In order to organize this analysis, we have grouped the molecules according to the number of carbon atoms in its structure: C_2H_n (ethane), C_3H_n (allene, propyne, cyclopropane, propene, and propane), C_5H_n (n-pentane), and C_6H_n (benzene, cyclohexane, and hexane).

1. Ethane (C_2H_6)

A great test case for our model potential calculations is the ethane molecule: it is the second molecule of the alkane family and, due to its relative simplicity, there are also previous SP calculations available [29]. Thus, in Fig. 3, we present our calculated ICS for positron elastic scattering from ethane, in the $S + \mathrm{V}_{\mathrm{CP}}$ approximation, compared with the earlier experimental TCSs and elastic ICS (SMC-SP) of Chiari *et al.* [19], the early calculations of Occhigrossi and Gianturco [36], and our more recent SP calculations [29].

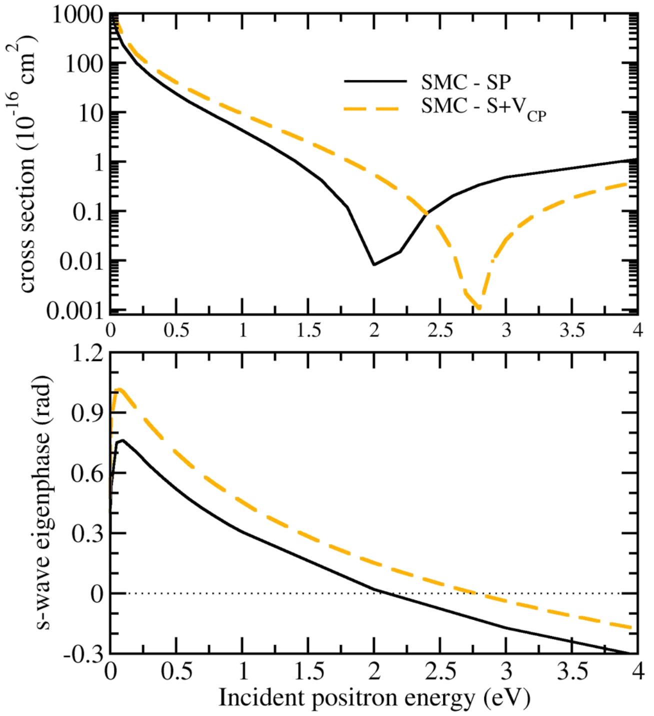

FIG. 4. Present s-wave cross section (top panel) and eigenphase (bottom) for positron scattering by ethane, compared with our previous SP calculations [29].

As seen in Fig. 3, our $S + V_{\mathrm{CP}}$ calculation has a higher magnitude in almost all energy ranges considered. In particular, as the impact energy goes toward zero, the elastic ICS in the present $S + V_{\mathrm{CP}}$ is more than twice our previous SP calculations, and closer to the experimental data of [19] for impact energies above 0.3 eV. At lower energies, both sets of SMC results overestimate the experimental TCSs, a behavior somewhat expected since the experimental data are underestimated due to the angular resolution of the apparatus [30]. Thus, even though we pushed to the limit of our computational capabilities in the SP calculations in [29], our current $S + V_{\mathrm{CP}}$ results, with the cutoff parameters obtained from hydrogen and methane molecules, seem to better describe the low-energy positron scattering by ethane.

In order to better understand the underlying physics in this low-energy range, in Fig. 4 we compare the s-wave cross sections and respective eigenphase between our previous SP and current $S + V_{\mathrm{CP}}$ calculations. These results are important to characterize the possible virtual or bound state for this molecule. Also, by analyzing the Ramsauer-Townsend minimum in the s-wave CS, we can assess how attractive is the resulting potential felt by the incoming positron.

As it is seen in Fig. 4, as the impact energy goes to zero, the s-wave CS is higher for the $S + V_{\mathrm{CP}}$ than the SP calculations. Also, the respective eigenphase indicates that this rise in the CS is due to a virtual state [37] (this will be further discussed in Sec. III C) and the Ramsauer-Townsend minimum is higher in energy for the $S + V_{\mathrm{CP}}$ when compared to the SP calculations. These are strong indications of a more attractive potential in the $S + V_{\mathrm{CP}}$ approximation.

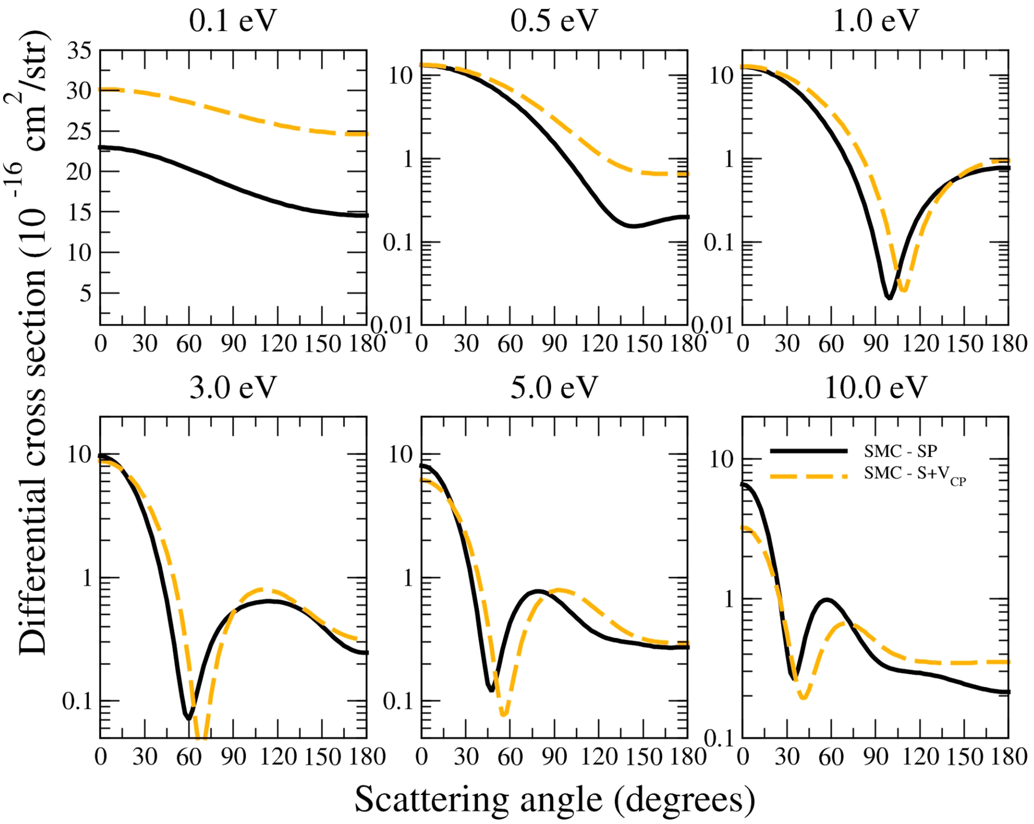

FIG. 5. DCSs for elastic positron scattering from ethane. Our $S + V_{\mathrm{CP}}$ (orange dashed line) results are compared with results from the earlier SMC-SP calculations of Frighetto *et al.* [29] (solid black line).

In Fig. 5 we compare our calculated results for the DCSs with the calculated results of Frighetto *et al.* [29]. Our $S + V_{\mathrm{CP}}$ approximation calculation seems to adequately describe the DCSs, providing the same oscillatory patterns as the SP approximation calculation. It is also noted that at 0.1 and 0.5 eV our $S + V_{\mathrm{CP}}$ calculation seems to provide more intense DCSs consistent with what is observed for the ICS. At 5.0 and 10.0 eV, our $S + V_{\mathrm{CP}}$ DCSs present lower magnitudes at lower scattering angles. The main reason for this difference is the fact that the SP calculations were carried out including additional functions in extra centers, which are important in coupling higher partial waves and key to describing low scattering angles.

2. Allene (C_3H_4)*, cyclopropane* (*c*-C_3H_6)*, propene* (C_3H_6)*, and propane* (C_3H_8)

In this section, we shall discuss positron scattering by hydrocarbon molecules presenting three C atoms. In particular, we will present and discuss our results for allene (C_3H_4), two isomers of C_3H_6, cyclopropane and propene, and propane (C_3H_8). The choice for these molecules is mainly due to the availability of measurements and/or calculations in the literature. Moreover, these molecules form an interesting set since they present C atoms in different hybridizations. In allene, two of the carbon atoms are in sp_2 hybridization and one carbon atom is in *sp* hybridization. In cyclopropane and propane, all carbons are in sp_3 hybridization, but whereas the former is a closed chain the latter is an open chain. Finally, propene presents two carbon atoms in sp_2 and one carbon atom in sp_3 hybridization.

In Fig. 6 we present our calculated $S + V_{\mathrm{CP}}$ integral cross sections for allene, propane, cyclopropane, and propene and compare with available calculations obtained in the SP approximation with the Schwinger multichannel method [20,31] and experimental total cross sections [38–40]. From this figure, it is readily seen that our $S + V_{\mathrm{CP}}$ calculations present very good agreement with the previous calculations for allene. It is worth mentioning that the previous SP calculation for allene employed several additional functions in extra chargeless centers and was the higher-level fully *ab initio* calculation by the time. This result for allene corroborates the accuracy of this model potential calculation, even though the computational cost was abruptly reduced. In the comparison with the C_3H_6 isomers, our results present the same tendency but are higher in magnitude in all energy ranges when compared to the previous SP calculations. Both theoretical calculations differ considerably from the experimental data at low impact energies, which is due to the poor angular resolution of the experimental apparatus [30]. The difference between the theoretical results can be associated with a more attractive potential described in the scattering process by the $S + V_{\mathrm{CP}}$ approximation.

In Fig. 7 we compare our calculated DCSs for cyclopropane with previous SMC-SP calculations from Nunes *et al.* [20]. Our $S + V_{\mathrm{CP}}$ approximation calculation provides the same oscillatory patterns as the previous SP calculation but with a much more intense DCS at the lower impact angles

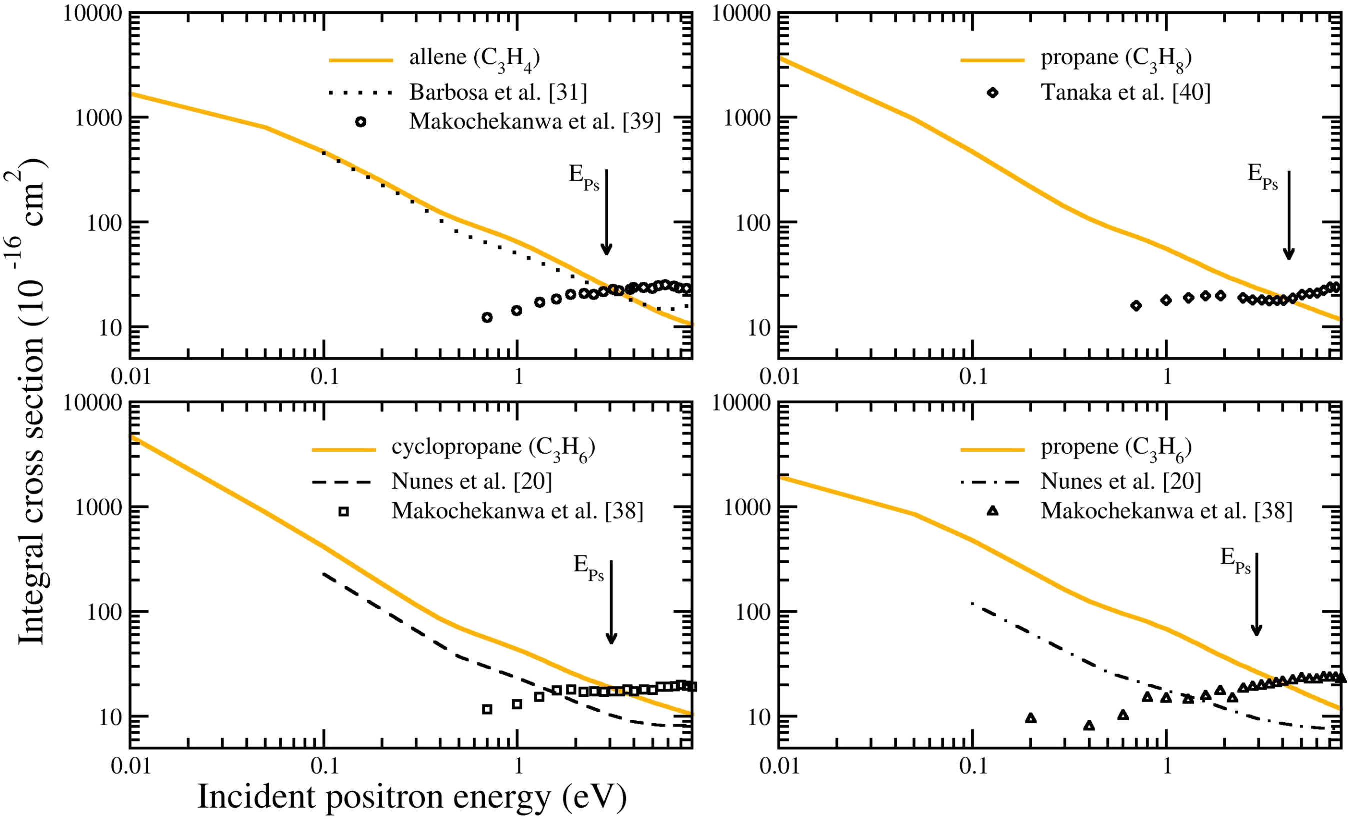

FIG. 6. ICSs for elastic positron scattering from allene, propane, cyclopropane, and propene. Our $S + V_{CP}$ (orange solid line) results are compared with previously calculated ICSs, when available, and measured TCSs. In each panel, the vertical arrow indicates the opening of the positronium channel at $E_{Ps} = 2.89$ eV [39] for allene, $E_{Ps} = 3.06$ eV [38] for cyclopropane, $E_{Ps} = 2.93$ eV [38] for propene, and $E_{Ps} = 4.30$ eV [41] for propane. See text for discussion

(<30°), which is indicative of a better description of the polarization effects in the positron-molecule dynamics. Despite not being shown here, similar results were obtained for the propene molecule.

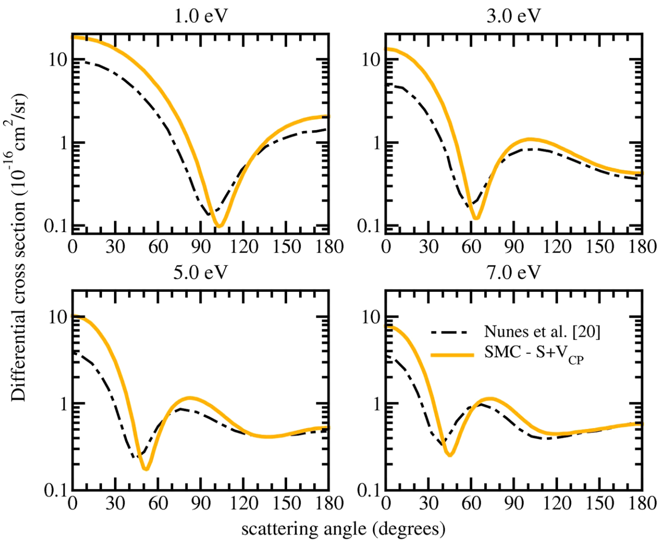

FIG. 7. DCSs for elastic positron scattering from cyclopropane. Our $S + V_{CP}$ (orange line) results are compared with the earlier SMC-SP results of Nunes *el al.* [20] (thin black dot-dashed line).

3. *n-pentane* (C_5H_{12})

N-pentane, C_5H_{12}, and its isomers isopentane and neopentane have been the subject of some theoretical and experimental studies on positron scattering, most of them aiming to identify the isomer effect among these targets [42,43]. Recently, in a joint theoretical and experimental work, we have studied positron-isopentane scattering, presenting calculated ICS and DCSs for elastic scattering, and measured total Ps formation and elastic differential cross sections [44]. Here, we present results for the *n*-pentane isomer of C_5H_{12}, which has all of its carbon atoms in the sp_3 hybridization.

In Fig. 8, we show the ICS for the elastic scattering of positron by *n*-pentane, in the $S + V_{CP}$ approximation. In the top panel we compare our calculated elastic ICS with previous calculations obtained with the independent atom model with screening corrected additivity rule (IAM-SCAR) [42] and the modified spherical complex optical potential (mSCOP) method [43] and measured TCS, from Trento University [42] for *n*-pentane. In the bottom panel, we compare our $S + V_{CP}$ results for *n*-pentane with our previous calculations and measured TCS, from the ANU group, for its isomer, isopentane [44]. From this figure, one can note that whereas our SMC-$S + V_{CP}$ calculations for *n*-pentane lie almost together with our previous calculations for isopentane there is a reasonable difference when comparing with previous calculations from Sinha and Antony, and Chiari *et al.*, in particular at lower

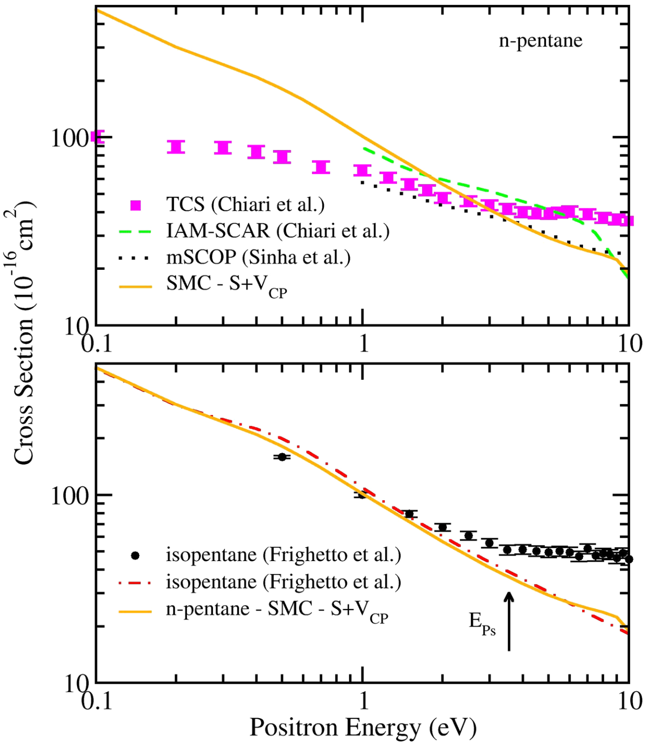

FIG. 8. Calculated ICS for elastic positron scattering by *n*-pentane. Top: our $S + V_{\mathrm{CP}}$ (orange solid line) results for *n*-pentane are compared with the earlier calculations for the same target obtained with the IAM-SCAR [42] (green dashed line) and mSCOP [43] (black dotted line) methods, and measured TCS, from Chiari *et al.* [42] (magenta squares). Bottom: our $S + V_{\mathrm{CP}}$ calculations for *n*-pentane compared with previous calculations (red dot-dashed line) and measurements (black circles), from Frighetto *et al.* [44] for isopentane. The vertical arrow corresponds to the energy at which the positronium channel opens ($E_{\mathrm{Ps}} = 3.55$ eV [42])

impact energies. Also at these energies, our $S + V_{\mathrm{CP}}$ calculations present better agreement with the more recent TCSs for isopentane. As the impact energy increases, our $S + V_{\mathrm{CP}}$ data rapidly decrease, being lower than the data of Chiari *et al.* As was observed in [28], this can be attributed to the poor description of higher partial waves of the $S + V_{\mathrm{CP}}$ data since the cutoff parameter was determined to better describe the very-low-energy regime. Also, since the Ps formation channel opens at 3.55 eV, we do not expect a good agreement between our CS and the experimental data, since our calculations do not include explicitly this channel and it can account for up to 50% of the TCS [45].

In Fig. 9 we compare elastic DCSs for *n*-pentane with previous calculations for isopentane, employing the same $S + V_{\mathrm{CP}}$ approximation, results obtained with the IAM-SCAR method [42], and the mSCOP formalism [43]. It is seen that our results present quite different oscillatory patterns than those of the IAM-SCAR and mSCOP formalisms, which could be associated with the limitations of these methods in this low-energy range. Regarding the comparison between both C_5H_{12} isomers, it is noted that the minima in the isopentane DCSs are more pronounced than those for *n*-pentane, mainly at 1.0 and 2.0 eV, which could be a signature of the isomer effect.

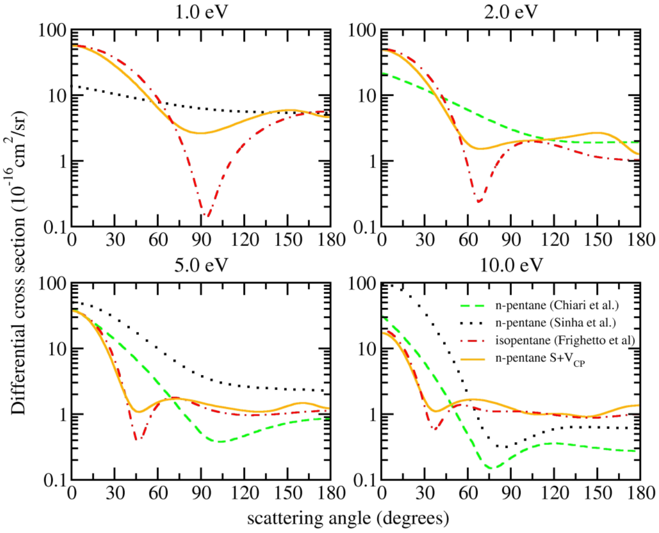

FIG. 9. DCSs for positron scattering from *n*-pentane. Our $S + V_{\mathrm{CP}}$ (orange solid line) results are compared with the earlier theoretical results of Chiari *et al.* obtained with the IAM-SCAR method [42] (red dashed line) and of Sinha and Antony obtained with the mSCOP formalism [43] (black dotted line). Our previous $S + V_{\mathrm{CP}}$ calculations for isopentane [44] are also shown.

4. *Hexane* (C_6H_{14})*, cyclohexane* (C_6H_{12})*, and benzene* (C_6H_6)

Finally, we now present the results for elastic positron scattering by the six carbon molecules hexane, cyclohexane, and benzene. Whereas hexane and cyclohexane are alkanes, and thus the calculations were carried out employing the optimal ρ value for the sp_3 hybridization of the C atom, benzene is an aromatic molecule, where all C atoms are in the sp_2 hybridization.

In Fig. 10 we present our $S + V_{\mathrm{CP}}$ calculations for cyclohexane and hexane and compare them with the available results for both molecules. For hexane, the only available data are measured total cross sections from Sueoka *et al.* [46]. The discrepancy between experiment and theory as the impact energy goes to zero is the same as previously observed for allene, propene, cyclopropane, and propane, and it is related to the poor angular resolution of the measurements [30]. In the same work, the authors also reported TCSs for positron-cyclohexane scattering, which are also shown in Fig. 10. For cyclohexane, there are also the *R*-matrix calculations of Karbowski *et al.* [47], and the measurements from the Trento experimental group [48,49], which in general present a better description of the low-energy scattering due to a better angular resolution of the experimental apparatus. There is a noticeable good agreement of the data from Karbowski *et al.* [47] and from the Trento group with our calculations for cyclohexane particularly for low scattering energies. Once again, for higher energies, the opening of the Ps formation channel (not included in our calculations) as well as the poor description of higher partial waves in the $S + V_{\mathrm{CP}}$ calculations can be responsible for the poorer agreement.

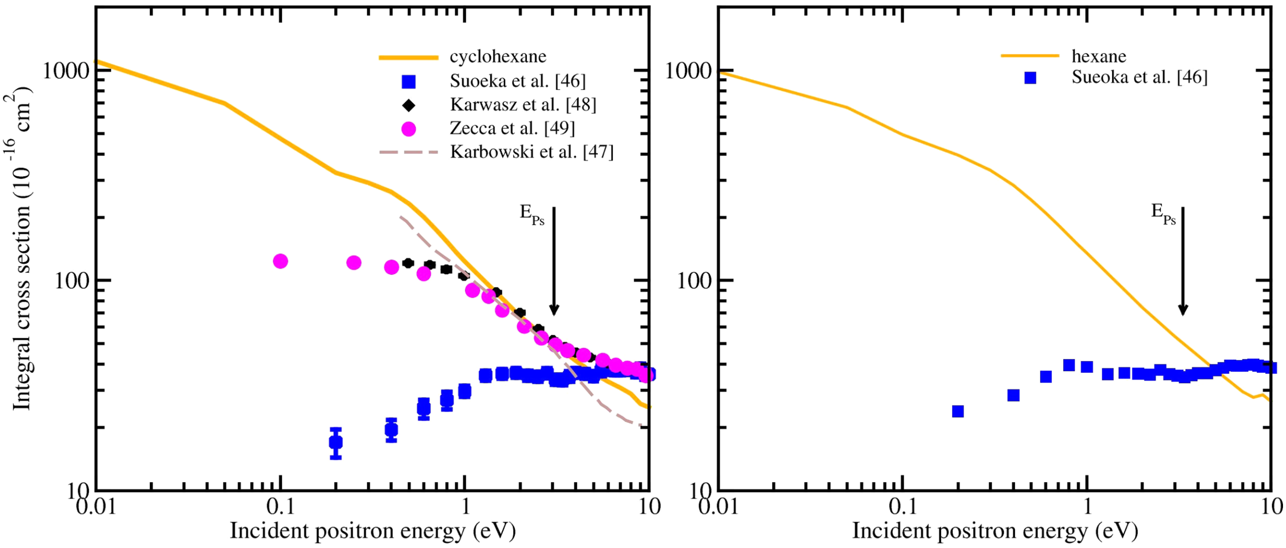

FIG. 10. Calculated ICS for elastic positron scattering by cyclohexane (left) and hexane (right). Our $S + V_{\mathrm{CP}}$ results are compared with the earlier theoretical result of Karbowski *et al.* [47], and with the experimental data of Sueoka *et al.* [46], Karwasz *et al.* [48], and Zecca *et al.* [49]. The vertical arrows indicate the opening of the positronium channel at $E_{\mathrm{Ps}} = 3.06$ eV for cyclohexane and $E_{\mathrm{Ps}} = 3.33$ eV for hexane [49].

In Fig. 11, we present our elastic ICS for positron-benzene scattering compared with the previously measured TCSs of Sueoka [50], Makochekanwa *et al.* [51], Karwasz *et al.* [48], and Zecca *et al.* [49]. We also compare our calculations with the earlier calculations of Occhigrossi and Gianturco [36] and of Barbosa *et al.* [21], with the SMC method and with the independent atom model with the screening corrected additivity rule method. Our $S + V_{\mathrm{CP}}$ calculation has a larger ICS magnitude when compared to the earlier calculations up until the Ps channel opens, presenting a better agreement with almost all experimental data except those from [51], due to the same reasons previously mentioned. It is worth mentioning the great improvement in our calculations when compared to the previous *ab initio* SP results, showing that this potential can provide reliable estimates.

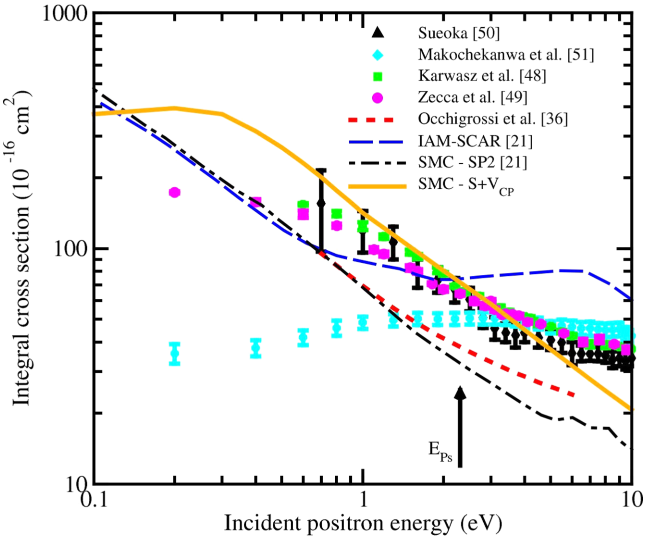

FIG. 11. ICS for positron scattering from benzene. Our $S + V_{\mathrm{CP}}$ (solid orange line) results are compared with the earlier theoretical results of Occhigrossi and Gianturco [36] and Barbosa *et al.* [21], obtained with the SMC method and with the IAM-SCAR method, and with the experimental data of Sueoka [50], Makochekanwa *et al.* [51], Karwasz *et al.* [48], and Zecca *et al.* [49]. The vertical arrow indicates the threshold for the positronium formation channel ($E_{\mathrm{Ps}} = 2.3$ eV [49]).

In Fig. 12 we compare our s-wave cross section and respective eigenphase with previous SMC-SP calculations from Barbosa *et al.* [21]. At lower impact energies, typically below 0.2 eV, our $S + V_{\mathrm{CP}}$ s-wave cross sections present a smaller magnitude when compared with the SP results. This behavior is associated with the existence of a more stable bound state in the $S + V_{\mathrm{CP}}$ calculation. This can be corroborated by the analysis of the SL. As the energy goes towards zero, the magnitude of the s-wave cross section goes with the square of the SL, whereas the binding energy can be calculated as $\varepsilon_B \approx \frac{1}{2(\mathrm{SL})^2}$ [37].

In Fig. 13 we compare our calculated elastic DCSs, in the $S + V_{\mathrm{CP}}$ approximation, with the previous calculations of Barbosa *et al.* [21], with the SMC method, and with the IAM-SCAR method. Our $S + V_{\mathrm{CP}}$ results present the same oscillatory patterns as the previous SP calculations but with a much more intense DCS at the low angle region (<30°). There is a clear difference between the oscillatory pattern of the DCSs calculated with the IAM-SCAR and those calculated with the SMC method, which could be associated with the limitations of the IAM-SCAR method in this low-energy range [21].

C. Virtual and bound states

When studying positron interactions with molecules, another important feature to be investigated is the possibility of a bound (or virtual) state formation, in particular, due to its relevance in the understanding of positron annihilation in the positron-molecule interaction. Usually, this phenomenon is identified in the behavior of the s-wave CS (hence the ICS)

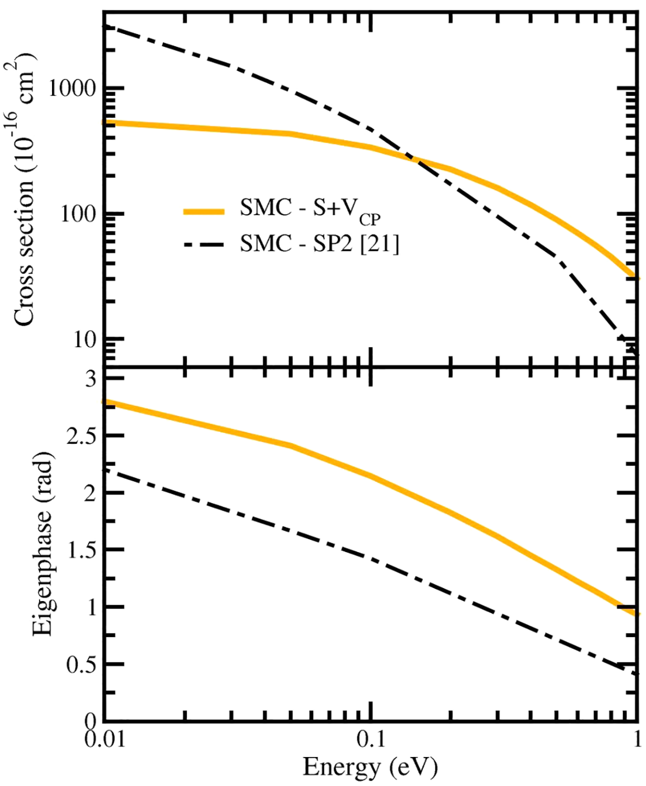

FIG. 12. s-wave cross section (top) and eigenphase (bottom) for elastic positron-benzene scattering compared with previous SMC-SP calculations of Barbosa *et al.* [21].

and eigenphase as the impact energy goes toward zero. For example, in Figs. 4 and 12 we have shown the s-wave cross sections and eigenphase for ethane and benzene, respectively. In both cases, the cross sections increase as the impact energy goes toward zero, but the assignment of this rising is given by the analysis of the s-wave eigenphase. When a bound state is expected, the s-wave eigenphase has a negative slope, whereas when a virtual state is expected, at very-low impact energies the s-wave eigenphase has a positive slope.

From the ICS presented in the previous sections, the great rise in magnitude as the impact energy goes to zero is clear. Thus, in Fig. 14 we present the corresponding s-wave eigenphase for each molecule of this paper, obtained in the $S + V_{\text{CP}}$ approximation. It is seen that for all unsaturated and bigger saturated hydrocarbons, the s-wave eigenphase seems to go to π and present a negative slope. This is indicative that a bound state takes place. For the smaller alkanes, in particular, methane and ethane, the positive slope of the eigenphase at lower energies is clear, indicating a virtual state.

Quantitatively one can assign whether a bound or virtual state is found by calculating the scattering length, which is defined as [52]

$$\text{SL} = \lim_{k\to 0} \frac{\tan[\delta_0(k)]}{k} \qquad (6)$$

where k is the positron momentum and $\delta_0(k)$ is the corresponding s-wave eigenphase [37]. If the SL is positive (negative) then a bound (virtual) state takes place.

Then, as mentioned earlier, we can obtain the bound or virtual state energy as $\varepsilon \approx \frac{1}{2(\text{SL})^2}$ [37]. In Table II we present the positron virtual or bound-state energies with the hydrocarbons studied in this paper, and compare with previous results from scattering *ab initio* calculations with the SMC method [20,21,29], with binding energy calculations of Swann and Gribakin [23], and with experimental measurements from Surko's group [22–25].

Initially, let us call attention to the bound (virtual) state energies calculated in the $S + V_{\text{CP}}$ and SP [29] for methane, ethylene, and acetylene. Since we found the cutoff parameter for the C atom that better fitted our SP calculations in the lower energies, we expected that the low-energy positron physics described in both calculations should be the same. And this is exactly what is seen here. For the other molecules, as can be seen in Table II, our calculations with the $S + V_{\text{CP}}$ approximation are able to predict bound states for most of the systems of interest, although for ethane and cyclopropane it still predicts the existence of a virtual state. For the other systems, the predicted bound-state energies are lower than the expected experimental value. Nonetheless, we can see quite an improvement concerning earlier SP approximation calculations in ethane, cyclopropane, and benzene. It is important to remark on the distinct difference in the calculated virtual

TABLE II. Positron (virtual) bound-state energies for the set of hydrocarbons studied in this paper. All energies are presented in units of meV. The positive (negative) values indicate a bound (virtual) state, and N.O. means not observed.

Molecule	$S + V_{\text{CP}}$ approximation	SP approximation	Swann and Gribakin [23]	Experimental
Methane	−151.330	−149.875 [29]	−3.021	N.O.
Ethylene	0.016	0.008 [29]	4.802	20 ± 8 [24]
Acetylene	0.763	0.689 [29]	−0.8408	⩾0 [23]
Ethane	−5.231	−23.260 [29]	−1.395	3 ± 3 [25]
Allene	21.275	2.785 (SP6) [31]		
Cyclopropane	−0.010	−26.638 [20]		16 ± 6 [25]
Propene	17.433			
Propane	4.419		14.33	16 ± 3 [25]
n-pentane	33.139			67 ± 4 [25]
Benzene	74.110	7.4 [21]		133 ± 5 [24]
Cyclohexane	37.383			82 ± 4 [25]
Hexane	42.910		85.85	94 ± 3 [23]

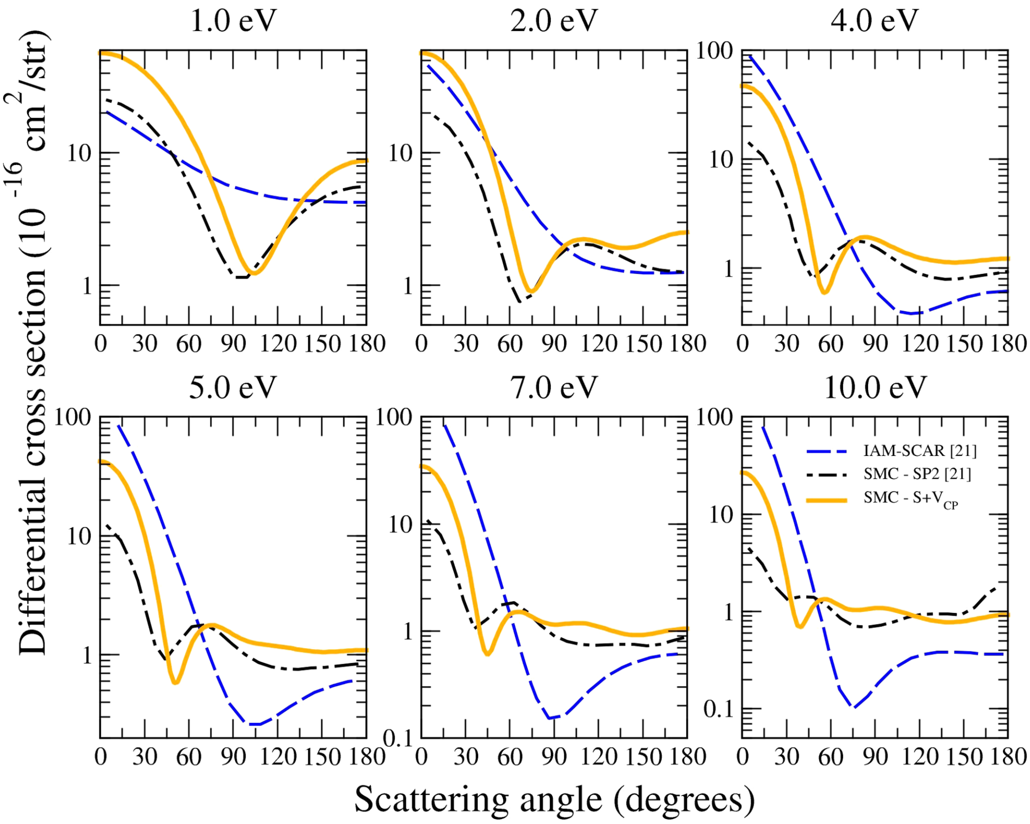

FIG. 13. DCSs for positron scattering from benzene. Our $S + V_{\mathrm{CP}}$ (orange line) results are compared with the earlier theoretical results of Barbosa *et al.* [21] obtained with the SMC method (thin black dot-dashed line) and IAM-SCAR (thin blue dashed line).

or bound-state energies between our current calculations and those of Swann and Gribakin [23]. Although the same structure for the model potential is used, our current calculations use a different method to calculate virtual or bound-state energies, different basis sets, and different empirical parameters than those of Swann and Gribakin [23]. For instance, their data were calculated by obtaining the cutoff parameter (equal for C and H) in order to obtain the experimental value of the bound state for larger molecules (such as propane and hexane) and then applying the same cutoff parameter for the rest. This is totally different from what we have performed, focusing on the atoms separately and in the *ab initio* *s*-wave

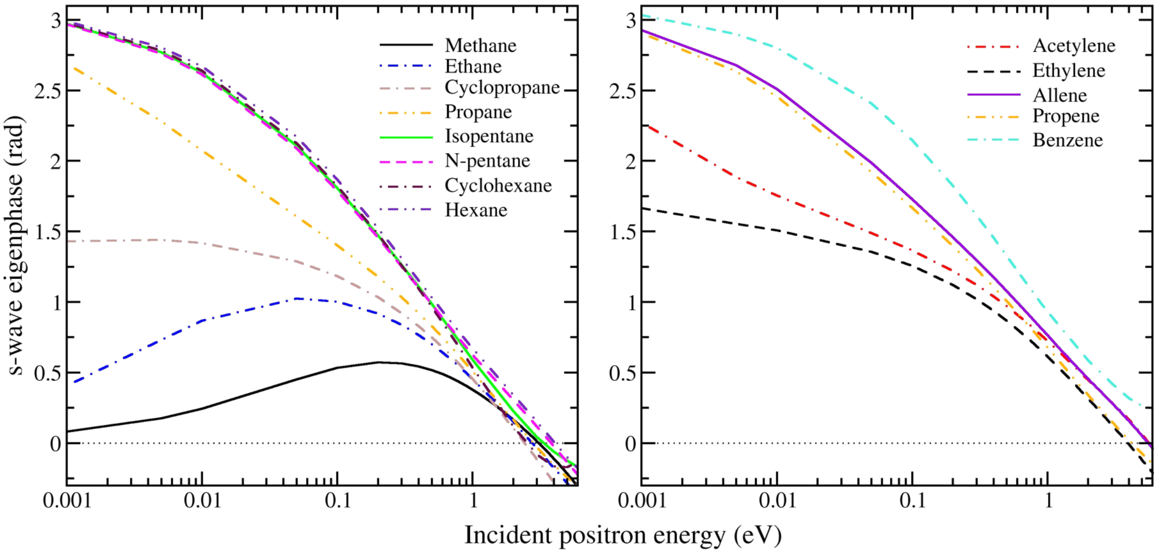

FIG. 14. *s*-wave eigenphase for elastic positron scattering from the molecules presented in this paper, obtained in the $S + V_{\mathrm{CP}}$ approximation. Saturated hydrocarbons are presented in the left panel, whereas the unsaturated ones are presented in the right panel. See text for discussion.

TABLE III. Number of most CSFs per symmetry used in the SP approximation and number of CSFs used in the $S + V_{CP}$ approximation.

Molecule	Number of most CSFs per symmetry used in the SP approximation	Number of CSFs used in the $S + V_{CP}$ approximation
Methane	23 384 [29]	85
Acetylene	17 013 [29]	92
Ethylene	16 983 [29]	118
Ethane	30 384 [29]	144
Allene	14 954 [31]	151
Cyclopropane	12 011 [20]	177
Propene	12 339 [20]	177
Benzene	15 425 [21]	276

scattering eigenphases. Hence, it is expected that their data would be closer to the experiment.

IV. SUMMARY

In this paper, we have presented calculations for elastic positron-molecule scattering employing the SMC method implemented with a correlation-polarization model potential. Initially, we have successfully determined the cutoff parameter for the carbon atom in different hybridizations by comparing with our previous *ab initio* SP calculations for the smaller alkane, alkene, and alkyne systems. Then, we have applied the same cutoff parameter to different hydrocarbons and obtained good and reliable cross sections. Besides that, we have also shown that our calculations support the existence of bound states for most hydrocarbons studied here, in agreement with experimental findings. This is a good indication that this cutoff parameter is only related to the atom and its hybridization and seems independent of the size of the hydrocarbon. Therefore, it can be used to generate reliable CSs for even bigger systems if desired.

It is also important to remark that the computational costs of the $S + V_{CP}$ approximation calculations are much cheaper than those of the SP approximation calculation; as an example we show in Table III the number of CSFs involved in each of the approximations. As can be seen, $S + V_{CP}$ approximation calculations require many fewer CSFs than SP approximation calculations, which in turn greatly decrease the size of the matrices involved in the calculation of the scattering amplitude in Eq. (3). This is quite significant as, for instance, the lower-upper decomposition used for the inversion of the denominator matrix $d_{\mu\nu}$ in Eq. (1) [28] has a complexity of $O(N^3)$ [53], where N is the number of CSFs involved in the calculation.

However, as mentioned in [54], better results could be achieved if one cutoff parameter per angular momentum is used. Our main focus in future works with the SMC method in the $S + V_{CP}$ approximation will be solving this issue and observing if the same cutoff parameter for one atom can be applied despite the size of the molecule it belongs to. In this sense, this tool can become extremely relevant to guide further experiments and investigations in positron interaction with molecules of considerable size.

ACKNOWLEDGMENTS

The authors acknowledge support from the Brazilian agencies Coordenação de Aperfeiçoamento Pessoal de Nível Superior (CAPES) and Conselho Nacional de Desenvolvimento Científico e Tecnológico (CNPq). A.S.B. and S.d'A.S. also acknowledge support from PESQUISA/PRPPG/UFPR. The authors acknowledge computational support from Prof. Carlos M. de Carvalho at LFTC-DFis-UFPR and at LCPAD-UFPR.

[1] W. N. Johnson, III, F. R. Harnden, Jr., and R. C. Haymes, The spectrum of low-energy gamma radiation from the galactic-center region, Astrophys. J. **172**, L1 (1972).

[2] N. Guessouum, R. Ramaty, and R. Lingenfelter, Positron annihilation in the interstellar medium, Astrophys. J. **378**, 170 (1991).

[3] H. Häkkinen, S. Mäkinen, and M. Manninen, Positron states in dislocations: Shallow and deep traps, Europhys. Lett. **9**, 809 (1989).

[4] S. Tanigawa, Defects in semiconductors observed by positron annihilation, Hyperfine Interact. **79**, 575 (1993).

[5] C. Hugenschmidt, U. Holzwarth, M. Jansen, S. Kohn, and K. Maier, Crystallization of silica studied by positron annihilation, J. Non-Cryst. Solids **217**, 72 (1997).

[6] G. P. Karwasz, A. Zecca, R. S. Brusa, and D. Pliszka, Application of positron annihilation techniques for semiconductor studies, J. Alloys Compd. **382**, 244 (2004).

[7] S. I. Ziegler, Positron emission tomography: Principles, technology, and recent developments, Nucl. Phys. A **752**, 679 (2005).

[8] R. E. Robson, M. J. Brunger, S. J. Buckman, G. Garcia, Z. L. Petrović, and R. D. White, Positron kinetics in an idealized PET environment, Sci. Rep. **5**, 12674 (2015).

[9] J. S. E. Germano and M. A. P. Lima, Schwinger multichannel method for positron-molecule scattering, Phys. Rev. A **47**, 3976 (1993).

[10] E. P. da Silva, J. S. E. Germano, and M. A. P. Lima, Z_{eff} according to the Schwinger multichannel method in positron scattering, Phys. Rev. A **49**, R1527(R) (1994).

[11] J. Tennyson, Electron-molecule collision calculations using the R-matrix method, Phys. Rep. **491**, 29 (2010).

[12] J. M. Carr, P. G. Galiatsatos, J. D. Gorfinkiel, A. G. Harvey, M. A. Lysaght, D. Madden, Z. Mašín, M. Plummer, J. Tennyson, and H. N. Varambhia, UKRmol: A low-energy electron- and positron-molecule scattering suite, Eur. Phys. J. D **66**, 58 (2012).

[13] V. Graves and J. D. Gorfinkiel, R-matrix calculations for elastic electron and positron scattering from pyrazine: Effect of the polarization description, Eur. Phys. J. D **76**, 43 (2022).

[14] M. C. Zammit, D. V. Fursa, J. S. Savage, I. Bray, L. Chiari, A. Zecca, and M. J. Brunger, Adiabatic-nuclei calculations of positron scattering from molecular hydrogen, Phys. Rev. A **95**, 022707 (2017).

[15] J. Hofierka, B. Cunningham, C. M. Rawlins, C. H. Patterson, and D. G. Green, Many-body theory of positron binding to polyatomic molecules, Nature (London) **606**, 688 (2022).

[16] C. M. Rawlins, J. Hofierka, B. Cunningham, C. H. Patterson, and D. G. Green, Many-body theory calculations of positron scattering and annihilation in H_2, N_2, and CH_4, Phys. Rev. Lett. **130**, 263001 (2023).

[17] A. Zecca, L. Chiari, E. Trainotti, A. Sarkar, S. d'A. Sanchez, M. H. F. Bettega, M. T. do N. Varella, M. A. P. Lima, and M. J. Brunger, Positron scattering from methane, Phys. Rev. A **85**, 012707 (2012).

[18] M. H. F. Bettega, S. d'A. Sanchez, M. T. do N. Varella, M. A. P. Lima, L. Chiari, A. Zecca, E. Trainotti, and M. J. Brunger, Positron collisions with ethene, Phys. Rev. A **86**, 022709 (2012).

[19] L. Chiari, A. Zecca, E. Trainotti, M. H. F. Bettega, S. d'A. Sanchez, M. T. do N. Varella, M. A. P. Lima, and M. J. Brunger, Cross sections for positron scattering from ethane, Phys. Rev. A **87**, 032707 (2013).

[20] F. B. Nunes, M. H. F. Bettega, and S. d'A. Sanchez, Positron collisions with C_3H_6 isomers, J. Phys. B **48**, 165201 (2015).

[21] A. S. Barbosa, F. Blanco, G. García, and M. H. F. Bettega, Theoretical study on positron scattering by benzene over a broad energy range, Phys. Rev. A **100**, 042705 (2019).

[22] J. A. Young and C. M. Surko, Feshbach-resonance-mediated annihilation in positron interactions with large molecules, Phys. Rev. A **77**, 052704 (2008).

[23] A. R. Swann, G. F. Gribakin, J. R. Danielson, S. Ghosh, M. R. Natisin, and C. M. Surko, Effect of chlorination on positron binding to hydrocarbons: Experiment and theory, Phys. Rev. A **104**, 012813 (2021).

[24] J. R. Danielson, S. Ghosh, and C. M. Surko, Enhancement of positron binding energy in molecules containing π bonds, Phys. Rev. A **106**, 032811 (2022).

[25] J. R. Danielson, S. Ghosh, Arthur-E. Baidoo, D. R. Witteman, and C. M. Surko, Positron binding to alkane molecules, Phys. Rev. A **108**, 032801 (2023).

[26] J. R. Machacek, E. K. Anderson, C. Makochekanwa, S. J. Buckman, and J. P. Sullivan, Positron scattering from molecular hydrogen, Phys. Rev. A **88**, 042715 (2013).

[27] A. R. Swann and G. F. Gribakin, Calculations of positron binding and annihilation in polyatomic molecules, J. Chem. Phys. **149**, 244305 (2018).

[28] F. F. Frighetto, A. S. Barbosa, and S. d'A. Sanchez, Implementation of a model potential in the Schwinger multichannel method to describe polarization in positron-atom and -molecule scattering: Studies for the noble-gas atoms, H_2 and N_2, Phys. Rev. A **108**, 012818 (2023).

[29] F. F. Frighetto, S. d'A. Sanchez, and A. S. Barbosa, Low-energy positron scattering by small hydrocarbons: methane, acetylene, ethylene, and ethane molecules, Eur. Phys. J. D **77**, 206 (2023).

[30] M. J. Brunger, S. J. Buckman, and K. Ratnavelu, Positron scattering from molecules: An experimental cross section compilation for positron transport studies and benchmarking theory, J. Phys. Chem. Ref. Data **46**, 023102 (2017).

[31] A. S. Barbosa, S. d'A. Sanchez, and M. H. F. Bettega, Bound state in positron scattering by allene, Phys. Rev. A **96**, 062706 (2017).

[32] A. R. Swann and G. F. Gribakin, Positron binding and annihilation in alkane molecules, Phys. Rev. Lett. **123**, 113402 (2019).

[33] K. J. Miller, Additivity methods in molecular polarizability, J. Am. Chem. Soc. **112**, 8533 (1990).

[34] https://cccbdb.nist.gov/.

[35] S. Tsuzuki, T. Uchimaru, and K. Tanabe, Conformational analysis of *n*-alkanes using density functional theory. Comparison with ab initio calculations, Chem. Phys. Lett. **246**, 9 (1995).

[36] A. Occhigrossi and F. A. Gianturco, Low-energy positron dynamics in small hydrocarbon gases, J. Phys. B **36**, 1383 (2003).

[37] C. J. Joachain, *Quantum Collision Theory* (North-Holland, Amsterdam, 1975).

[38] C. Makochekanwa, M. Hoshino, H. Kato, O. Sueoka, M. Kimura, and H. Tanaka, Electron and positron scattering cross sections for propene and cyclopropane, Phys. Rev. A **77**, 042717 (2008).

[39] C. Makochekanwa, H. Kawate, O. Sueoka, M. Kimura, M. Kitajima, M. Hoshino, and B. Tanaka, Total and elastic cross-sections of electron and positron scattering from C_3H_4 molecules (allene and propyne), Chem. Phys. Lett. **368**, 82 (2003).

[40] H. Tanaka, Y. Tachibana, M. Kitajima, O. Sueoka, H. Takaki, A. Hamada, and M. Kimura, Total cross sections of electron and positron collisions with C_3F_8 and C_3H_8 molecules and differential elastic and vibrational excitation cross sections by electron impact on these molecules, Phys. Rev. A **59**, 2006 (1999).

[41] K. Floeder, D. Fromme, W. Raith, A. Schwab, and G. Sinapius, Total cross section measurements for positron and electron scattering on hydrocarbons between 5 and 400 eV, J. Phys. B **18**, 3347 (1985).

[42] L. Chiari, A. Zecca, F. Blanco, G. García, and M. J. Brunger, Experimental and theoretical cross sections for positron scattering from the pentane isomers, J. Chem. Phys. **144**, 084301 (2016).

[43] N. Sinha and B. Antony, Theoretical study of positron scattering from pentane isomers, Chem. Phys. Lett. **713**, 282 (2018).

[44] F. F. Frighetto, L. Chiari, P. S. Sullivan, S. J. Buckmann, M. H. F. Bettega, S. d'A. Sanchez, A. S. Barbosa, and M. J. Brunger, Joint theoretical and experimental study on positron scattering by isopentane, Eur. Phys. J. D **78**, 7 (2024).

[45] C. K. Kwan, W. E. Kauppila, S. Nazaran, D. Przybyla, N. Scahill, and T. S. Stein, Positron-molecule scattering experiments, Nucl. Instrum. Methods Phys. Res., Sect. B **143**, 61 (1998).

[46] O. Sueoka, C. Makochekanwa, H. Tanino, and M. Kimura, Total cross-section measurements for positrons and electrons colliding with alkane molecules: Normal hexane and cyclohexane, Phys. Rev. A **72**, 042705 (2005).

[47] A. Karbowski, G. P. Karwasz, M. Franz, and J. Franz, Positron scattering and annihilation in organic molecules, Acta Phys. Pol. B **51**, 207 (2020).

[48] G. P. Karwasz, D. Pliszka, R. S. Brusa, and C. Perazzolli, Low energy cross-sections for positron interactions with cyclic hydrocarbons, Acta Phys. Pol. A **107**, 666 (2005).

[49] A. Zecca, N. Moser, C. Perazzolli, A. Salemi, and M. J. Brunger, Total cross sections for positron scattering from benzene, cyclohexane, and aniline, Phys. Rev. A **76**, 022708 (2007).

[50] O. Sueoka, Total cross section measurements for positron and electron scattering on benzene molecules, J. Phys. B **21**, L631 (1988).

[51] C. Makochekanwa, O. Sueoka, and M. Kimura, Comparative study of electron and positron scattering from benzene C_6H_6 and hexafluorobenzene C_6F_6 molecules, Phys. Rev. A **68**, 032707 (2003).

[52] M. A. Morrison, Interpretation of the near-threshold behavior of cross sections for e-CO_2 scattering, Phys. Rev. A **25**, 1445 (1982).

[53] S. Lee and C. Y. Lee, A faster LU decomposition for parallel C programs, Korean J. Com. Appl. Math. **3**, 217 (1996).

[54] J. Mitroy and I. A. Ivanov, Semiempirical model of positron scattering and annihilation, Phys. Rev. A **65**, 042705 (2002).